Asociación Argentina
de Mecánica Computacional

Mecánica Computacional Vol XL, págs. 329-338 (artículo completo)
F.A. Avid, L.C. Bessone, P. Gamazo, J.J. Penco, M.A. Pucheta, M.A. Storti (Eds.)
Concordia, 6-9 Noviembre 2023

NUMERICAL INVESTIGATION OF BUCKLING OF STRUCTURAL INSULATED PANEL UNDER IN-PLANE LOADING

Cindy G. Wozniuk[a], Eduardo M. Sosa[b] and Rossana C. Jaca[c]

[a] *WOZ Ingeniería, Illia 1024, 8300 Neuquén, Argentina. geraldwoz@gmail.com*

[b] *Department of Mechanical and Aerospace Engineering, West Virginia University 1306 Evansdale Dr., Morgantown, 26505, West Virginia, United States. eduardo.sosa@mail.wvu.edu*

[c] *Departamento de Ingeniería Civil, Facultad de Ingeniería, Universidad Nacional del Comahue, Buenos Aires 1400, 8300 Neuquén, Argentina. rossana.jaca@fain.uncoma.edu.ar*

Keywords: Buckling, Structural Insulated Panel, Finite element analysis, Compression Loading.

Abstract. Structural insulated panels (SIP) are thriving in the construction industry as an alternative to traditional materials. These panels considerably improve construction times compared to conventional wet systems. Its implementation in varied designs results in versatile structures with more comfortable and cooler interior environments, translating into significant energy savings for its inhabitants. These panels are made of a composite material. They are typically comprised of two outer layers and a core layer. The outer layers are formed by wooden flakes mixed with a phenolic and polyurethane adhesive pressed at high temperature and pressure. The core middle layer is formed by high-density expanded polystyrene and bonded to the outer layers by high-strength adhesives. Various mechanical tests are usually conducted on isolated panel modules to ensure their good structural behavior. This work presents details of a finite element model created to analyze the structural behavior of an isolated module subjected to in-plane compression. The panel is modeled with a multipurpose finite element code and includes linear buckling analysis (LBA) and geometric nonlinear analysis (GNLA) for the evaluation of buckling loads and nonlinear behavior. Modeling results are compared to the experimental results to validate the model's features and behavior so it can be used in future analyses involving three-dimensional configurations created from the combination of multiple panels.

1 INTRODUCTION

In the past few years, construction systems have evolved considerably, with new alternatives appearing to replace traditional systems and becoming the preferred option. Among those alternatives, the structural insulated panels (SIP) offer a composite material with distinctive mechanical and thermal properties. Each panel typically comprises two outer layers formed by wooden flakes mixed with a phenolic and polyurethane adhesive pressed at high temperature and pressure, known as Oriented Strand Board (OSB), and a core layer formed by high-density expanded polystyrene (EPS) (Amran et al., 2020; LP Building Products). The core layer is bonded to the outer layers by a high-strength adhesive, and some variants replace the expanded polystyrene core with an injected polyurethane core. Different panel thicknesses can be achieved by changing the core thickness. Customized thermal properties can be obtained depending on the thermal needs or the construction location where the panels are used (walls, mezzanine, ceiling) (Rojas, 2018). The SIP system originated in 1935 at the Forest Products Laboratory (FLP) in Madison, Wisconsin, USA. FLP engineers created the first pieces of plywood and hardwood sheeting to form a structurally load-bearing section of a wall. However, the design contained no insulation making it unsuitable for architectural resolutions. In 1952, the first core of rigid expanded polystyrene was created, and manufacturing developed during the 1960s. During the 1970s, more and more builders began to use them because of the numerous advantages they present (Amran et al., 2020). This constructive system is predominant in the United States (especially in Northwestern states), Canada, northern European countries, Japan, and, more recently, it has been gradually adopted in Chile and Argentina.

One of the main advantages of the SIP constructive system is its thermal efficiency. The panels have insulation incorporated into their core, which reduces the energy requirements for heating and/or cooling the habitable space. A lower energy consumption reduces the emissions of CO2 to the atmosphere, reduces the environmental impact, and, therefore, becomes a sustainable construction system (Cárdenas et al., 2015). Another advantage is the structural capacity to resist high loads horizontally and vertically and their earthquake-resistant behavior. The constructions' lightness also allows for the expansion of several height levels (Rammer and Williamson, 2020). Moreover, implementing the SIP constructive system considerably improves construction times because the panels can be installed at any time of the year and in any climate without degrading their structural or thermal qualities. Typically, these panels are combined with laminated wood to reinforce the joints between modules, mezzanines, ceilings, and lintels to create high-strength structures (CIRSOC 601, 2016). The SIP constructive system typically sits on a foundation made of reinforced concrete, although a raised metal frame structure can also be designed (CIRSOC 201, 2005; CIRSOC 301, 2005).

Various mechanical tests are usually carried out on isolated panel modules in order to ensure their structural behavior, in-plane compression (Santarelli and P. Manzione, 2016; Kermani, 2006; Yang et al., 2012), shear (Rubilar, 2012), bending tests (Calquín, 2011; Kermani, 2006; Yang et al., 2012), as well as including impact tests (Chen and Hao, 2015). Typically, these tests are carried out in a single panel with different testing setups and machines. This study reports the results of one of them, and it is focused on analyzing the structural behavior of a single panel subjected to in-plane compression (Santarelli and Manzione, 2018). The evaluation is based on experimental measurements carried out on a single panel to determine its maximum loading capacity and deformation. A numerical analysis is implemented by modeling the panel using a general multipurpose finite element simulation package (Abaqus, 2017). Modeling results are compared to the experimental

results to validate the model's features and behavior so that it can be used in future analyses involving three-dimensional configurations created by combining multiple panels.

2 MATERIALS AND METHODS

2.1 Panel Configuration

The panel considered for this study is 1.22 m wide and 2.44 m high. The two OSB outer layers are 11 mm, and the EPS core layer is 68 mm thick. The total panel thickness is 90 mm. The three layers are bonded with a high-strength structural adhesive and pressed at high temperatures to obtain the composite panel.

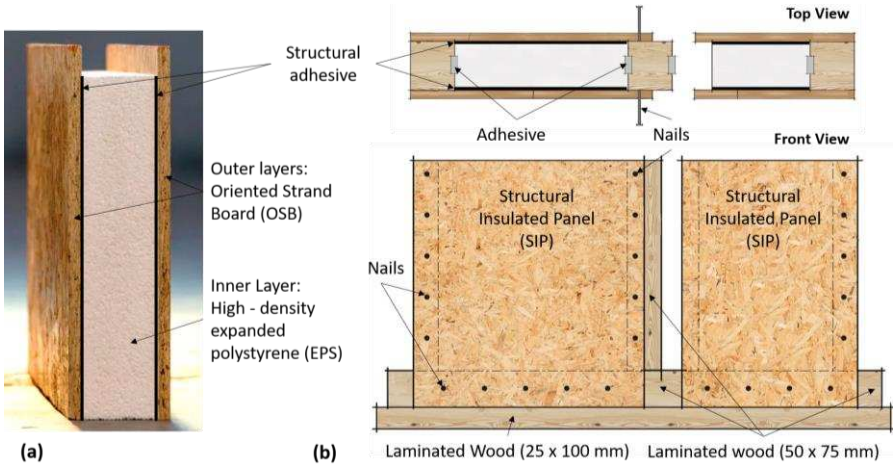

Figure 1. (a) Basic configuration of a Structural Insulated Panel (SIP); (b) Top and front views of integrated panels.

Figure 1(a) illustrates the main layer configuration, and Figure 1(b) the integration of two panels with a surrounding wooden frame (typically comprising 50 mm by 75 mm pieces) bonded by adhesives and nails in the perimeter of the panels. The wooden frame improves the bond between modules to obtain the three-dimensional configurations desired in the architectural designs. In addition to the surrounding frame, a 25 mm x 100 mm wooden base is placed at the bottom of the panels to connect the panels to the concrete foundation.

2.2 Experimental Setup

Figure 2(a) shows an overview of the experimental setup implemented for in-plane compression. An individual panel was placed in a vertical position and subjected to the in-plane compressive load applied by a hydraulic actuator through a load-distributing beam placed on the top edge of the panel. The compression load was applied incrementally at a rate of 10 kN/min. The hydraulic actuator was connected to a custom-made steel frame on one end and a 300-kN load cell on the other end. The top and bottom steel beams provided a simply supported boundary condition to both ends of the panel. Vertical displacements were measured digitally with four linear variable differential transformers (LVDT) (Figure 2(b)). An additional transducer was also used to measure the lateral (out-of-plane) displacement at the mid-height of the panel (Figures 2(c)). For each load increment, the in-plane displacement and the lateral deflection were measured and recorded for post-processing. Three panels were tested with this configuration, and test results are presented along with numerical simulations in Section 3.

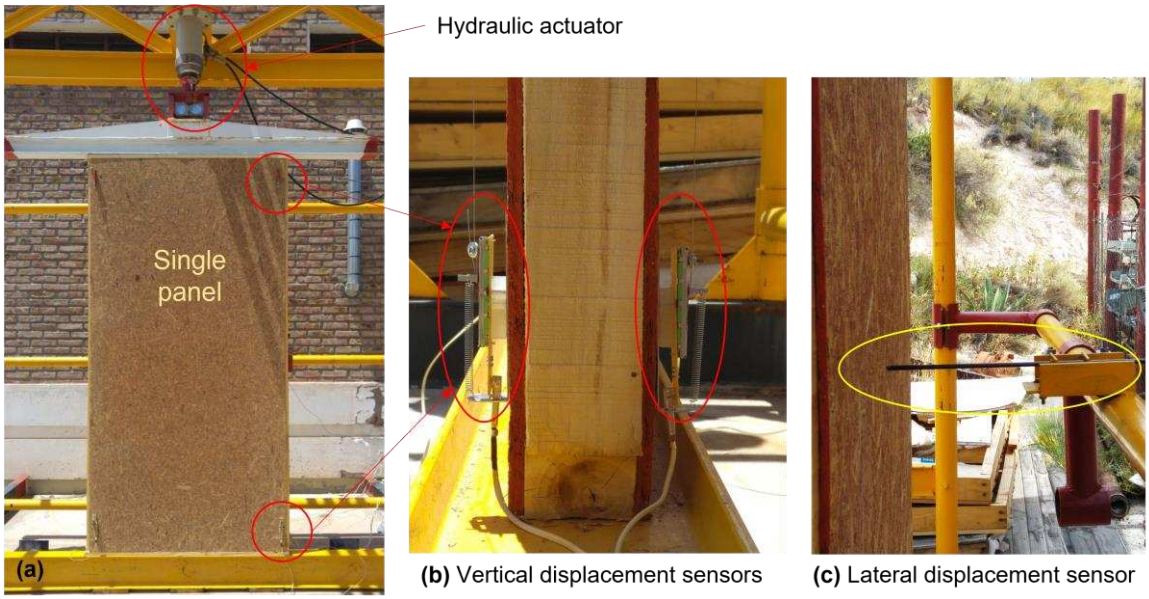

Figure 2: Overview of the experimental setup for in-plane compression tests.

2.3 Finite Element Model Setup

The panel configuration and experimental setup described in the previous sections were utilized to create a finite element model of the panel subjected to in-plane compression. The model was created with the Simulia/Abaqus simulation suite (Abaqus, 2017). The model included the following characteristics:

(a*) Parts and assembly*. The panel model had two OSB panels, a core EPS inner layer, and a wooden frame. The core inner layer is surrounded by the wooden frame and covered by the OSB panels, as shown in Figure 3(a).

(b) *Interactions*. The OSB panels are linked to the EPS panel via a cohesive contact model that simulates the presence of the structural adhesive. The perimeter of both OSB panels is connected to the wooden frame via discrete rigid ties that mimic the presence of nails spaced every 10 cm. The top edges of the OBS panels and the top surface of the wooden frame are coupled to a reference point (RP) created to simulate the point of load application. These interactions are illustrated in Figure 3(b).

(c) *Load and boundary conditions*. The bottom surface of the full SIP panel is assumed to have pinned boundary conditions (no translations, but rotations allowed). A concentrated force of 1 kN is applied as a reference force for buckling analysis to calculate the eigenvalues and buckling modes. This reference force is applied in the vertical direction and located at the reference point coupled to the top edge. For the nonlinear analysis, a prescribed displacement of 3 mm is applied in the downward vertical direction (U2) and concentrated at the reference point coupled to the top edge. The loading and boundary conditions are shown in Figure 3(c).

(d) *Elements and mesh*. All the parts are discretized using three-dimensional, 8-node, linear hexahedral (brick) elements (C3D8R) with reduced integration and hourglass control. The total panel geometry contained a total of 3,824 elements. The resulting meshed configuration is shown in Figure 3(c).

(e) *Material properties*. OSBs are usually considered orthotropic materials, and their material parameters are defined for longitudinal and transversal directions. The engineering constants summarized in Table 1 were extracted from (LP Building Products). Implementing continuous 3D solid elements in Abaqus required calculating the generalized orthotropic

material parameters (D_{ijkl}) (Abaqus, 2017). In this research, the Poissons' ratios were assumed as zero, and the resulting D_{ijkl} values are summarized in Table 1. The EPS inner layer was considered isotropic with a modulus of elasticity of E_{EPS} = 1 MPa and ν = 0.1 (García et al., 2016). The wooden frame was assumed to be made of pine wood, with an isotropic modulus of elasticity of E_W = 6,800 MPa and ν = 0.36 determined from static bending tests (Green et al., 1999). The bonding strength of the adhesive material corresponding to an OSB-EPS-OSB under tension was extracted from (Franklin Adhesives & Polymers) S_{ADH} = 0.145 MPa. This strength value and a separation of 0.1 mm were adopted for estimating a linear cohesive contact model defined by a maximum nominal stress of 0.145 MPa, an elastic stiffness K = 0.145 / 0.1 = 1.45 MN/mm, and a damage evolution controlled by the energy per unit of area defined by the area under the traction-separation diagram for a displacement at a separation of 0.2 mm and equal to A_{energy} = 0.0145 MN.mm/mm^2 (Abaqus, 2017).

(f) *Analyses*. This study conducted two types of analyses. First, a linear buckling analysis (LBA) was implemented to estimate the eigenvalues corresponding to the first and second buckling modes and for the initial estimation of the critical buckling load. Then, a geometric nonlinear analysis (GNLA) was implemented to obtain the nonlinear loading trajectory under an imposed vertical displacement applied at the reference point.

Engineering Constants [MPa]	Orthotropic Material Parameters (D_{ijkl}) [MPa]
E_1 = 6,399	D_{1111} = 6,399
E_2 = 1,316	D_{2222} = 1,316
E_3 = 100	D_{3333} = 100
G_{12} = 1,080	D_{1122} = 0
G_{13} = 50	D_{1133} = 0
G_{23} = 50	D_{2233} = 0
$\nu_{12} = \nu_{21} = 0.0$	D_{1212} = 1,080
$\nu_{23} = \nu_{32} = 0.0$	D_{1313} = 50
$\nu_{31} = \nu_{13} = 0.0$	D_{2323} = 50

Table 1: OSB panel material properties (LP Building Products; Abaqus, 2017).

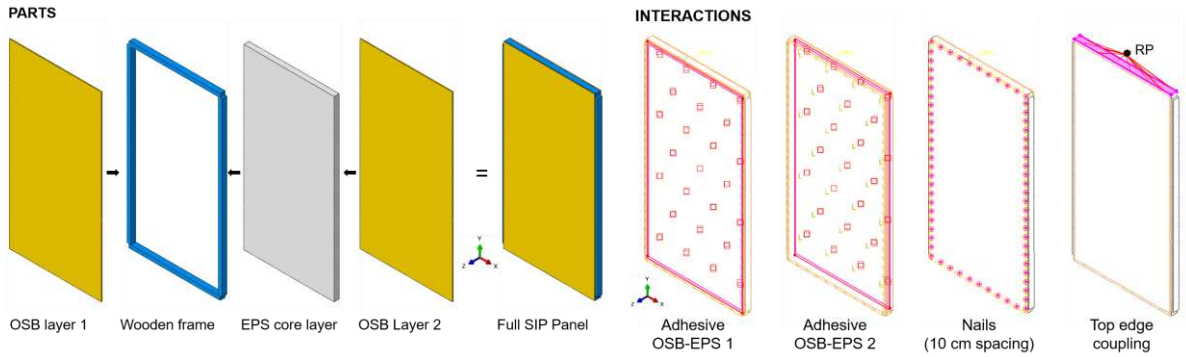

(a) (b)

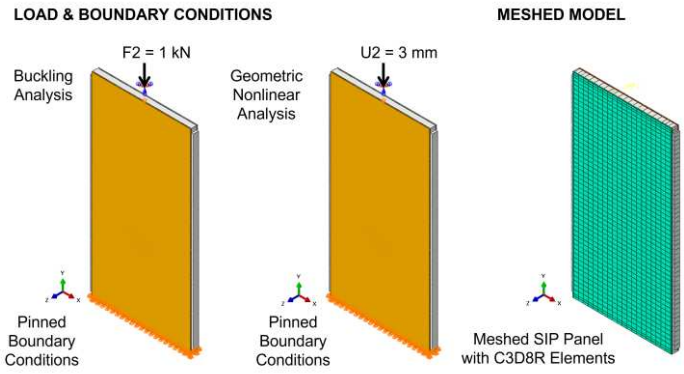

(c)

Figure 3. Finite element model setup. (a) Parts; (b) Interactions. RP: Reference Point; (c) Loading, boundary conditions, mesh.

3 RESULTS AND DISCUSSION

Three panels were tested under in-plane loads as described in Section 2.2. Each panel was loaded to failure, and Table 2 summarizes maximum load, maximum in-plane and out-of-plane displacements, and failure modes. The average maximum in-plane load was 149.4 kN, the average in-plane displacement was 2.4 mm, and the average maximum out-of-plane displacement was 12.2 mm. The load-displacement curves illustrated in Figure 4(a) show that panels #1 and #3 had similar stiffness, while panel #2 seemed stiffer than the others. Figure 4(a) also shows that a quadratic polynomial (n = 2) regression function seem to fit better (R^2 = 0.89) all the experimental data than a linear model (R^2 = 0.73). Regarding lateral displacement, panels #2 and #3 displayed similar maximum out-of-plane displacements (~9 mm). At the same time, panel #1 nearly duplicated the deformation of the other two (~18 mm), as also shown in the lateral displacement trajectories compiled in Figure 4(c). The average maximum values and the load-displacement curves were used as a reference for comparison with results obtained from the finite element simulations.

Results corresponding to the LBA indicated that the first eigenvalue corresponding to the lowest critical load was 154.51 kN, which is 3.4% higher than the average maximum load shown in Table 2. The corresponding first buckling mode included a primary central lobe flanked by two small ones in the opposite direction, as shown in Figure 5(a). The shape of this first mode resembles the buckling failure mode observed in the experiments.

Sample	Max. Load [kN]	Max. Axial Displacement [mm]	Max. Lateral Displacement [mm]	Failure Mode
Panel #1	146.4	2.69	17.77	Buckling
Panel #2	131.2	0.95	9.49	Buckling
Panel #3	170.7	3.44	9.19	Frame Failure
Average	149.4	2.4	12.2	
Std. Dev. (SD)	19.9	1.3	4.9	
COV = Avg./SD	13%	54%	40%	

Table 2: Summary of experimental results (Santarelli and Manzione, 2018).

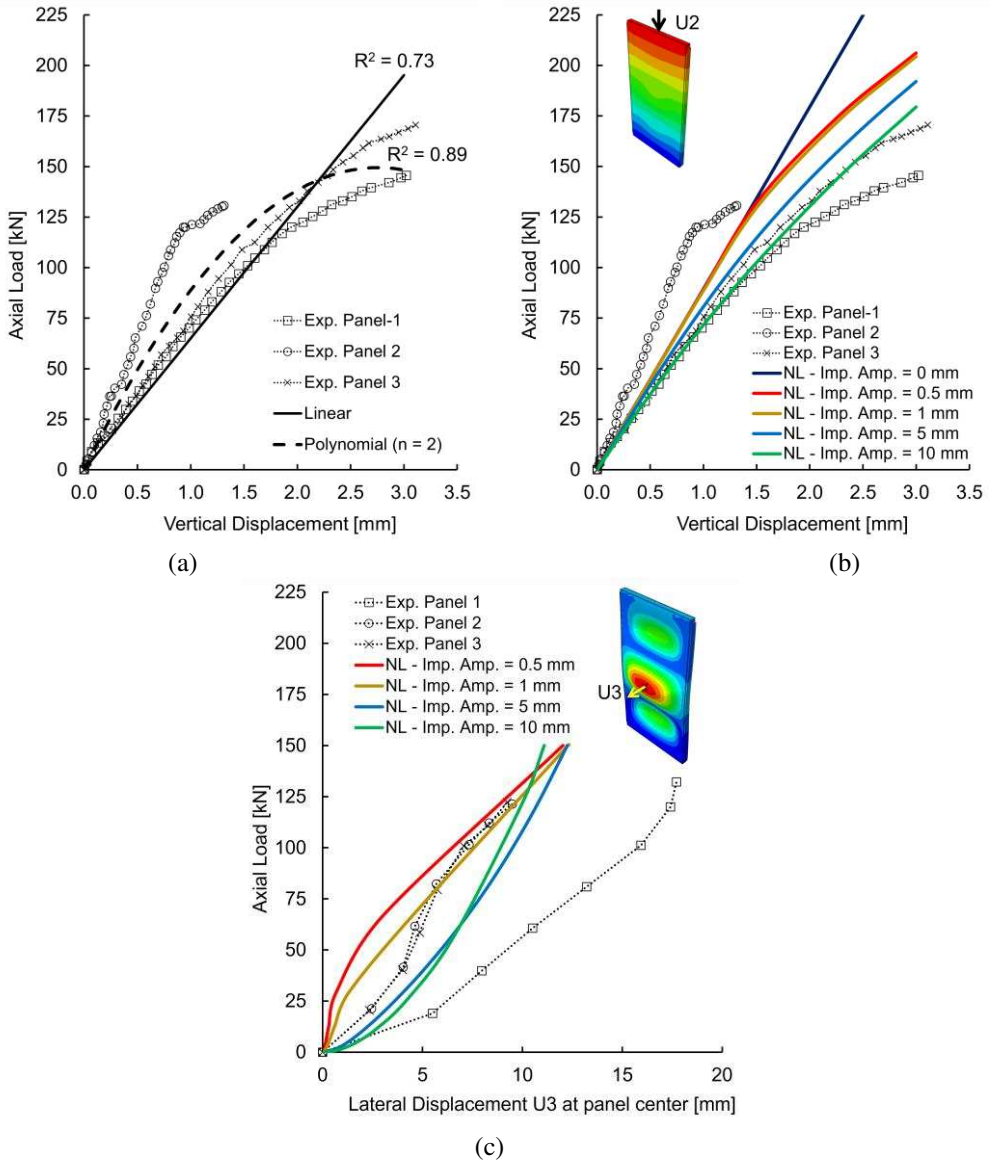

Figure 4. (a) Summary of experimental axial load vs. vertical displacement; (b) Experimental vs. Simulation for axial load and vertical displacement; (c) Experimental vs. Simulation for axial load and lateral displacement.

On the other side, the nonlinear trajectories obtained from the GNLA are presented in Figure 4(b) alongside the experimental results for in-plane loading. For a perfectly straight panel, with no imperfections and undamaged bonding between surfaces and uniform material properties, the behavior is linear. Theoretically, the panel could reach a maximum in-plane load of about 225 kN for an axial displacement (U2) of ~2.5 mm. However, in the actual panels, some imperfections originated from slight differences in manufacturing tolerances, non-uniform material properties, and small eccentricities during loading, among other factors that can deviate the panel from the ideal or nominal geometric configuration.

One way to account for these imperfections is to introduce small-amplitude geometric imperfections into the original geometric configuration. Typical shapes adopted for imperfections are some buckling modes obtained from the LBA. In this study, we introduced the shape of the first buckling mode scaled at four levels: 0.5, 1, 5, and 10 mm, which correspond to 5%, 9%, 45%, and 90% of the OSB nominal thickness (11 mm), respectively.

The resulting trajectories calculated, including these levels of imperfections, are presented in Figure 4(b) and compared to the curves obtained experimentally. Results indicate that for slight imperfections (0.5 and 1 mm), the behavior remains linear until about 125 kN. Then it becomes nonlinear until reaching a maximum load of about 204 kN for a maximum displacement of 3 mm. When the imperfection amplitude increased to 5 or 10 mm, the global stiffness of the panel decreased, and the maximum loads reached for a 3-mm maximum axial displacement were 192 kN and 179 kN, respectively, which approximate better the maximum loads measured experimentally.

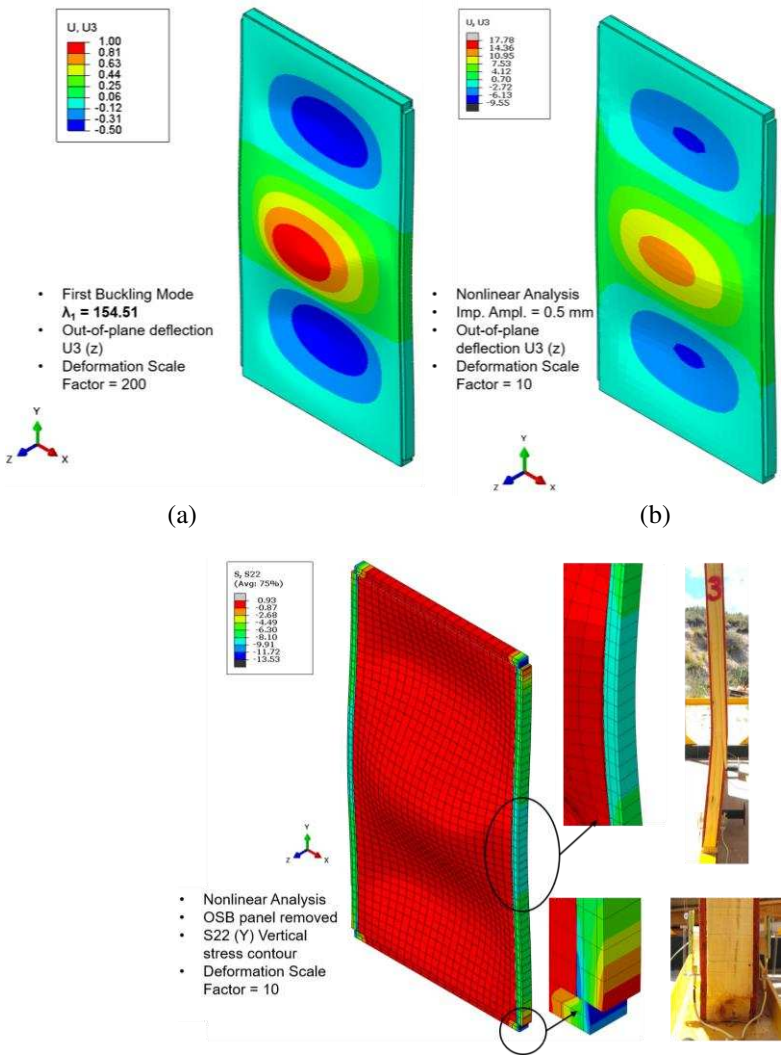

Figure 5. (a) First buckling mode; (b) Nonlinear analysis deflected shape; (c) Vertical stress contour from GNLA.

Simulation results for out-of-plane (U3) displacement trajectories are presented in Figure 4(c) alongside the experimental measurements at the center of the panels. An example of the deflected shape obtained from the GNLA is shown in Figure 5(b). Similar to the response seen for the axial displacements, the initial imperfection amplitude controls the out-of-plane displacement trajectories obtained from the simulations. For imperfections of 0.5 and 1 mm, the lateral displacement is initially minimal (< 2 mm) and then increases rapidly to reach a maximum of about 10 mm for an axial load of 150 kN, which is similar to the values achieved

by panels #2 and #3 (see Table 2). On the contrary, when the imperfection amplitude is relatively large, like 5 or 10 mm, the lateral displacements continue to increase until reaching a magnitude of about 12 mm at a load of 150 kN. Note that the shape of the experimental trajectories followed by panels #2 and #3 seem to follow a double curvature. This shape suggests that in the simulations, a combination of the first and second modes included as initial imperfection would better represent the trajectory observed in the experiments.

Figure 5(c) shows the normal stress distribution along the panel's vertical axis (y). As expected, the panel is subjected to a compressive stress uniformly distributed across the panel's width and partly transmitted through the wooden frame's vertical components. The stress contour also shows the regions of stress concentrations at the corners of the frame as well as stresses in the central region of the vertical legs, where failure was observed in one of the experimental panels. These results provide valuable information to elucidate how the load is transferred to the foundation and the influence of the stiffness of the panel in relation to the stiffness of the surrounding frame.

Finally, simulation results also showed no delamination between the OSB external layers and the core EPS layer, suggesting that the bonding strength provided by the adhesive was able to withstand the in-plane loading. However, further analysis would be necessary to investigate the panel load-carrying capacity as the adhesive degrades as a function of time and environmental conditions.

4 CONCLUSIONS

Experimental evaluations and finite element analyses were carried out to analyze the structural behavior of a structural insulated panel subjected to an in-plane compression load. Experimental results indicate that the panels fail largely by buckling, and the finite element simulation models can reproduce the structural behavior in two ways. First, the linear buckling analysis can estimate the critical buckling load and buckling mode in close agreement with the average values and shape obtained experimentally. Second, the geometrically nonlinear model can reasonably capture the loading and displacement trajectories observed experimentally, as well as the effect of the presence of geometric imperfections in the load-carrying capacity of the panels.

Overall, the finite element model with the features and techniques selected for analysis reasonably captured the experimental results obtained for a single panel and became a valuable prediction tool for reproducing other loading scenarios for SIP panels. Further parametric studies would be needed to analyze the variation of structural behavior as material properties and bonding characteristics change, and to understand the interaction among multiple panels under different loading configurations.

Acknowledgments. The authors are grateful to SECYT-UNCo for providing access to the experimental data (Santarelli and P. Manzione, 2016) and (Santarelli and P. Manzione, 2018) used in this study.

REFERENCES

Amran, Y.H.M., El-Zeadani, M., Leed, Y.H., Lee, Y.Y., Murali, G., and Feduik, R., Design innovation, efficiency and applications of structural insulated panels: A review. *Structures,* 27:1358-1379, 2020.

Calquín, P.V., Mechanical tests on a structural thermo-insulating panel (SIP) of 89 mm thick with EPS core and 9.5 mm OSB facings, PART 2: Bending test, Report N°666685-02, Faculty of Medical Sciences and Mathematics of Chile, 2011.

Cárdenas, J.P., Muñoz, E., Riquelme, C. and Hidalgo, F., Simplified life cycle assessment applied to structural insulated panel homes. *Construction Engineering Magazine*, 30(1):1-5, 2015.

Chen, W. and Hao, H., Performance of structural insulated panels with rigid skins subjected to windborne debris impacts – Experimental investigations. *Construction and Building Materials*, 77:241–252, 2015.

CIRSOC 201, *Argentine Regulation of Concrete Structures*. Research Center of National Safety Regulations for Civil Works. Buenos Aires, 2005.

CIRSOC 301, *Argentine Regulation of Steel for Buildings*. Research Center of National Safety Regulations for Civil Works. Buenos Aires, 2005.

CIRSOC 601, *Argentine Regulation for Wooden Structures*. Research Center of National Safety Regulations for Civil Works. Buenos Aires, 2016.

Franklin Adhesives & Polymers. "ReacTITE EP-980 Product Data Sheet". Online at: www.franklinadhesivesandpolymers.com.

García, N.P., Anguas, P.G., Salazar, A.P., Hidalgo, R.J. and Mondragón, F.C., Evaluación de las propiedades mecánicas del poliestireno expandido". *Instituto Mexicano del Transporte*, Publicación Técnica No. 476, 2016.

Green, D.W., Winandy, J.E. and Kretschmann, D.E., Chapter 4: Mechanical Properties of Wood, Forest Products Laboratory. Wood handbook—Wood as an engineering material. Gen. Tech. Rep. FPL–GTR–113. Madison, WI, US, 1999.

Kermani, A., Performance of structural insulated panels. *Proceedings of the Institution of Civil Engineers Structures & Buildings*, 159(SB1):13–19, 2006.

LP Building Products, SIP Systems Practical Construction Manual LP. LP Building Solutions, Santiago, Chile.

Rammer, D.R. and Williamson, T., Performance of Structural Insulated Panel Walls under Seismic Loading. Forest Service, Forest Products Laboratory, Research Paper FPL-RP-704, 2020.

Rojas, C.A.R., *Technical analysis of the use of SIP panels in the construction of single-family houses*. Thesis, Technical University Federico Santa Maria, King Baduino of Belgium, 2018.

Rubilar, G.S., Mechanical tests on a structural thermo-insulating panel (SIP) of 89 mm thick with EPS core and 9.5 mm OSB facings, Part 4: Horizontal load test, Report N°729465-04, Faculty of Medical Sciences and Mathematics of Chile, 2012.

Santarelli, E. and Manzione, P., Mechanical Tests of Structural Panels. Report 16/16GEPSyN, Department of Applied Mechanics, Universidad Nacional del Comahue, 2016.

Santarelli, E. and Manzione, P., Mechanical Tests of Structural Panels. Report 02/18GEPSyN, Department of Applied Mechanics, Universidad Nacional del Comahue, 2018.

Simulia/Abaqus. Abaqus User's Manual, Version 2017. Dassault Systèmes, Providence, RI; 2017.

Yang, J., Li, Z. and Du, Q., An Experimental Study on Material and Structural Properties of Structural Insulated Panels (SIPs). *Applied Mechanics and Materials*, 147:127-131, 2012.